

Formation of Gadolinium Doped Ceria Oxide Thin Films by Electron Beam Deposition

Giedrius LAUKAITIS^{1*}, Julius DUDONIS¹, Darius MILČIUS²

¹Physics Department, Kaunas University of Technology, Studentų 50, LT-51368 Kaunas, Lithuania,

²Materials Testing and Research Laboratory, Lithuania Energy Institute, Breslaujos 3, LT-44403 Kaunas, Lithuania

Received 06 October 2006; accepted 30 December 2006

Gadolinium doped ceria oxide (GDC) thin films were grown evaporating $(\text{Ce}_{0.9}\text{Gd}_{0.1})\text{O}_{1.95}$ ceramic powder by using e-beam deposition technique. Operating technical parameters that influence thin film properties were studied. The GDC thin films (2 μm – 3 μm of thickness) were deposited on two different types of substrates: porous NiO-YSZ (nickel oxide – yttrium stabilized zirconium) and Alloy 600 (Fe-Ni-Cr). The influence of electron gun power on thin film structure and surface morphology were investigated by X-ray diffraction and scanning electron microscopy. It was found that electron gun power (changed in the range of 0.66 kW – 1.05 kW) has the influence on the crystallite size (it varied between 7.6 nm – 14.3 nm) of GDC thin films and decreased linearly increasing e-beam gun power.

Keywords: electron beam deposition, GDC (gadolinium doped ceria oxide) thin films, microstructure, solid-oxide fuel cells (SOFC).

INTRODUCTION

CeO_2 -based ceramics are known for their wide range of applications. CeO_2 (ceria) is used in abrasives, pigments, catalyst, oxygen-ion-conducting solid electrolytes, and oxygen sensors [1]. However, the major interest in ceria-based ceramics has focused on their application as SOFCs (Solid Oxide Fuel Cells) [2]. Ceria-based ceramics are ionic conductors and are highly oxygen-conductive when subjected to temperatures of around 600 °C.

Recently, an intensive investigation has been done to reduce the operating temperature of SOFC down to 500 °C. Traditional SOFC with YSZ as electrolytes places considerable constraints on materials, which can be used for interconnections and balance-of-plant due to the high operating temperature (around 1000 °C), hence limits commercial development of SOFC. Therefore, it is desirable to reduce SOFC operating temperature to an intermediate temperature, while still maintaining the power density achieved at high temperature. For this purpose, either more conductive or thinner electrolyte is needed [3]. Ceria based solid solutions have been regarded as the most promising electrolytes for intermediate temperature SOFCs (IT-SOFC) because of their ionic conductivity is higher than YSZ at 600 °C (yttrium stabilized zirconium). The ionic conductivity of ceria has been extensively investigated with respect to different dopants (e.g. Ca_{2+} , Sr_{2+} , Y_{3+} , La_{3+} , Gd_{3+} , and Sm_{3+}) and dopant concentration [2]. It is generally accepted that Gd_{3+} or Sm_{3+} – doped ceria exhibits the highest conductivity due to the small association enthalpy between dopant cation and oxygen vacancy in the fluorite lattice [2 – 3]. In addition, decreasing the thickness of the electrolyte further reduces the resistance to ionic transport, resulting in an even lower operating temperature of SOFCs [3 – 7]. The low-temperature operation provides

an economic benefit through possible replacement of some of the expensive ceramic components of the cell by relative cheaper metallic alternatives. It can also eliminate problems caused by the reaction of the electrolyte with other cell components, lower degradation problems, less thermal mismatch [4, 6]. Furthermore, the interfacial losses of doped ceria electrolyte with cathode and anode are also lower than those of YSZ [6].

Several techniques have been employed to prepare the doped ceria oxide thin films. The techniques mainly include vapor processing methods such as chemical vapor deposition (CVD), electrochemical vapor deposition (EVD), metal-organic CVD (MOCVD), sputtering, plasma spray, etc. [8 – 10]. Each of the vacuum deposition techniques suffer from relatively high equipment cost and complexity, especially when compared to traditional methods of manufacture that include tape casting, tape calendaring, electrophoretic deposition, screen printing, and transfer printing, among others. Despite these challenges, vacuum methods offer a number of unique advantages. Very thin, fully dense layers can be produced on either porous or dense substrates, which may enable higher power densities to be achieved. Films can be formed at temperatures much lower than required in traditional ceramic processing. This does not allow unwanted interfacial reactions. Vacuum methods are also well suited to the formation of interlayers, where small grain sizes and thin layer thickness are required. Among the most unique aspects of vacuum deposition is the ability to produce unique structures that are not otherwise achievable [10].

In the present work, GDC electrolyte thin films were deposited using e-beam deposition technique on different types of substrates. Electron beam gun power and substrates types were changed in order to understand the influence of it on the formed GDC thin films texture, crystallite size, and homogeneity.

*Corresponding author. Tel.: +370-37-300303; fax: +370-37-456472.
E-mail address: gielauk@ktu.lt (G. Laukaitis)

EXPERIMENTAL

GDC thin films (2 μm – 3 μm of thickness) were deposited on different substrates: porous Ni-YSZ, and Alloy 600 (Fe-Ni-Cr). The experimental measurements of the thin film thickness were performed using weight method by employing precise (10^{-9} kg) microbalances. The substrates were cleaned in an ultrasonic bath (in pure acetone) before deposition. The EB-PVD technique was used for the experiment. All deposition experiments were performed at room temperature. More details of the technical parameters of the used technique are presented in [11]. Cubic phases of gadolinium doped ceria ($\text{Ce}_{0.9}\text{Gd}_{0.1}\text{O}_{1.95}$ ceramic nano-powder (99.9 % purity based on trace metal analysis, 5 nm – 10 nm particles of powder) were used as evaporation materials. Before deposition GDC powder was pressed to the pallets. The residual gas pressure in the vacuum chamber was 4×10^{-3} Pa. The distance between the electron gun and the substrate was fixed at 250 mm.

The film structure was analyzed by X-ray diffraction (XRD) (DRON – UM1 with standard Bragg-Brentan focusing geometry with an error of 0.01°) in a 10° – 80° range using the $\text{Cu K}\alpha$ ($\lambda = 0.154059$ nm) radiation. The crystallite size d of GDC thin films was estimated from the Scherrer's equation and using XFIT program with Voigt function modeling [12 – 13]. A Scanning Electron Microscope (SEM, JSM5600) was used to investigate the microstructure of the GDC thin films.

RESULTS AND DISCUSSIONS

The XRD diffraction patterns of the pressed GDC powder are presented in Fig. 1. It shows that the positions of the Bragg peaks are typical for the cubic $\text{Gd}_{0.1}\text{Ce}_{0.9}\text{O}_{1.95}$ (according to Crystallographica Search-Match, Version 2). XRD peaks of GDC thin films indicate sharp (111) and minor (200), (220), (311) and (222) orientations when cubic phase GDC powder as evaporation material is used. These GDC thin films repeat the crystal structure of the chosen evaporated material at all electron gun powers (Fig. 1).

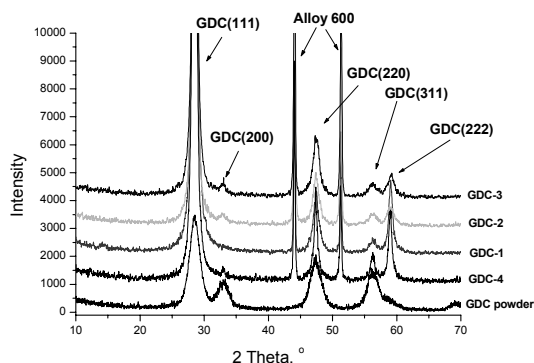


Fig. 1. XRD patterns of pressed GDC powder and GDC thin films deposited on Alloy 600 (Fe-Ni-Cr) substrates at different e-beam gun powers: GDC-4 – 0.66 kW, GDC-1 – 0.75 kW, GDC-2 – 0.9 kW, GDC-3 – 1.05 kW

The growth rate of the film during deposition could be increased by increasing e-beam gun power [11] and it has the influence on the crystallite size of the deposited GDC

thin films. By changing e-beam gun power it is possible to control the crystallite size. Crystallite size (Fig. 2) decreases linearly from 14.3 nm to 7.6 nm with the increase of e-beam gun power from 0.66 kW to 1.05 kW (the growth rate increases from 2.6 nm/s to 3.4 nm/s respectively). The lowest crystallite size is found to be for the e-beam gun power equal to 1.05 kW. It could be caused that during the e-beam deposition and increasing e-beam gun power the vapour stream consists of bigger amount of the small clusters of nanocrystalline powder. These clusters could be the initial growing stages influencing the thin film structure. The existence of the clusters in the vapour stream could be caused by expulsion of the material by the local electric field or explosive evaporation caused by the pores in the pressed GDC pallets which are in the evaporator. The same effect is found in the arc plasma thin film deposition [14]. GDC thin films crystal orientation corresponds to the requirements for good ionic conductivity of GDC electrolytes [1 – 5].

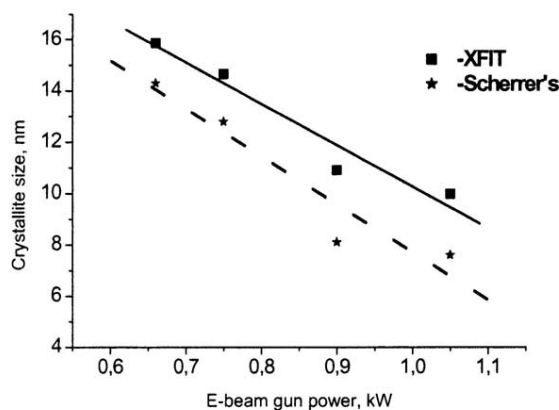


Fig. 2. Dependence of crystallite size (extracted from XRD data using XFIT-Voigt modeling and Scherrer's equation) on e-beam gun power for GDC thin films formed on Alloy 600 (Fe-Ni-Cr) substrates

The porosity of the substrate influences the morphology of the films substantially [15]. However, one of the main parameter which determines the film morphology is the substrate temperature during the thin film deposition. The microstructure of thin films can be roughly predicted using the Movchan and Demchishin or the Thorton structure diagrams [16 – 17]. In our case, EB deposited GDC thin film microstructure on porous substrates corresponds to the Zone 1 where the processing temperature normalized to the melting point of the coating material (T/T_m) is lower than 0.3. Using flat substrates (Alloy 600) the morphology of the surface region of thin films has a crystalline columnar texture with all columnar grains oriented in the same direction, namely perpendicular to the substrate, and with a predominantly open microporosity. The microstructure consists of parallel columns with gaps in between. The GDC thin films deposited on porous substrates consist of columns with “feathery” structure (Fig. 3). GDC thin films have a large number of interfaces, grain boundaries, nanoporosity and randomly oriented grains. When the vapour flux arrives on the substrate at oblique incidence, the resultant films are

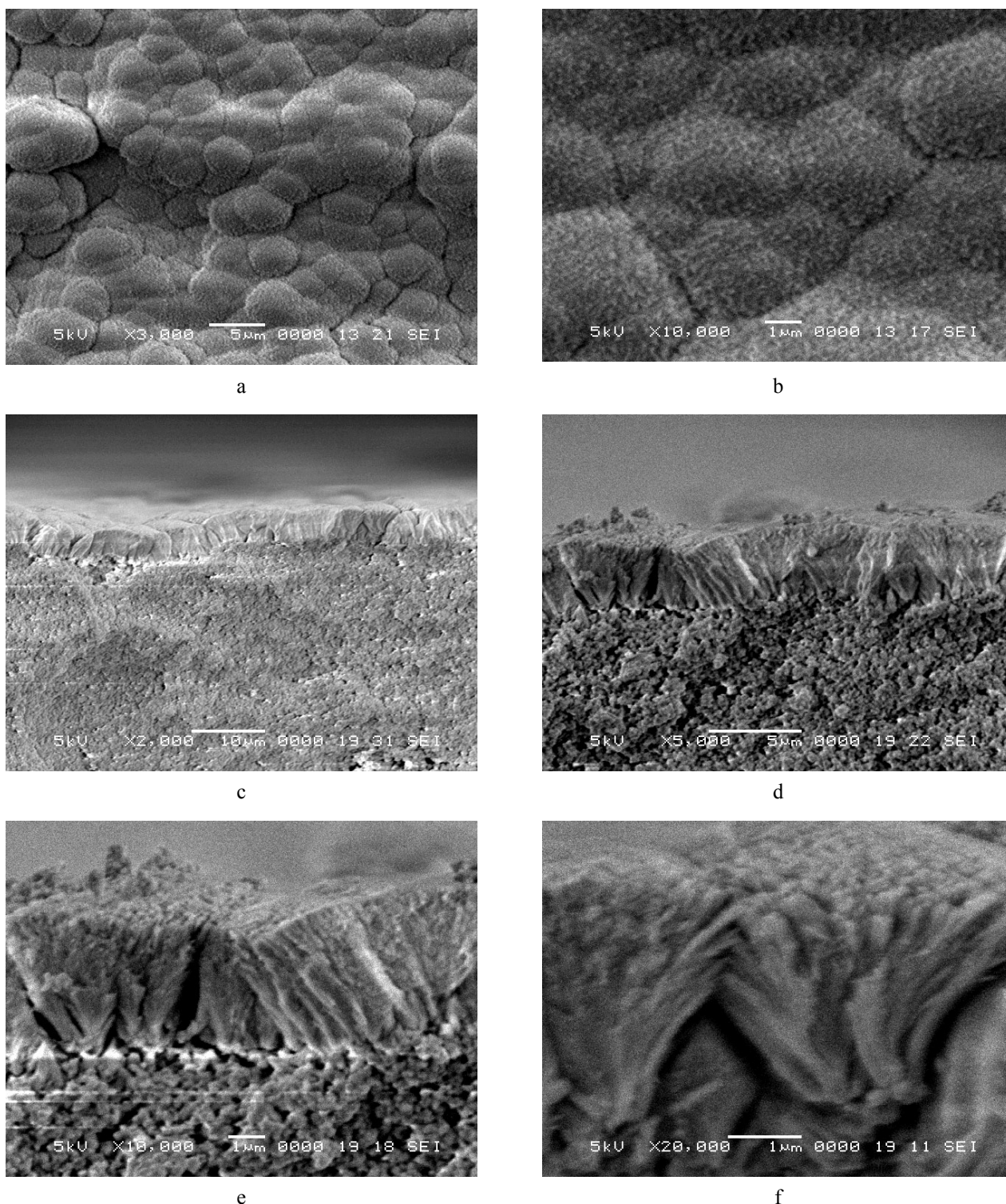
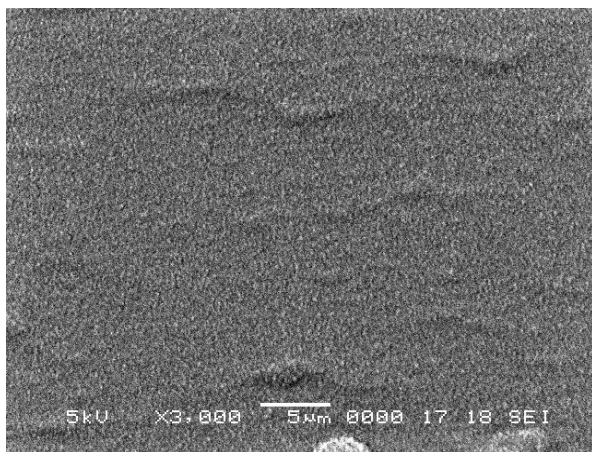


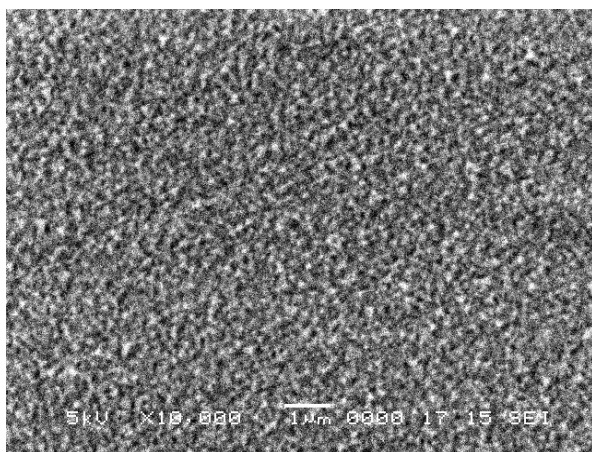
Fig. 3. SEM images at different magnitudes of the surface (a, b) and cross section (c, d, e, f) of GDC thin films deposited at $T = 293$ K with a e-beam gun power $P = 0.9$ kW on porous NiO-YSZ substrates

composed of columns that grow inclined towards the source flux. The individual columns have a larger diameter near the top surface and a smaller diameter near the GDC/substrate interface. The large column near the top surface consists of many fine columns of hundreds nanometers (Fig. 3), while columns near the interface consist of finer structures. Ceramic particles are oriented in different directions on the surface of porous substrates. For this

reason the vapour flux impinges at an angle of incidence in the range of $\alpha = 0^\circ$ to approximately 70° (measured with respect to substrate normal). That could be caused “feather” structures and the columns are mostly connected with their neighbors. In the case of flat substrates the columns are isolated from each other (Fig. 4). The same effect is found when a glancing angle deposition (GLAD) technique was used [18].



a



b

Fig. 4. SEM images of the surface of GDC thin films deposited at $T=293$ K with a e-beam gun power $P=0.9$ kW on porous Alloy 600 (Fe-Ni-Cr) substrates (at different magnitudes – a, b)

CONCLUSIONS

XRD results shows that the main dominating crystallite orientation of the GDC thin film repeats the characteristics of the used powder. The e-beam gun power (respectively the growth rate) influences the crystallite size of the obtained GDC thin films and it decreases linearly from 14.3 nm to 7.6 nm. Results show that GDC material starts to evaporate in the different type of clusters from the evaporant at the high e-beam gun power. The microstructure of EB-PVD deposited thin films depends on the type of substrate (flat or porous) used: deposited GDC thin films have a crystalline columnar texture with all columnar grains oriented in the same direction (perpendicular to the substrate) and isolated from each other when flat substrates (Alloy 600) are used; GDC thin films deposited on porous substrates consist of columns with a “feathery” structure, and the columns are connected with their neighbors.

Acknowledgement

Lithuanian State Science and Studies Foundation has supported this work.

REFERENCES

1. **Godinho, M. J., Gonçalves, R. F., Santos, L. P. S, Varela, J. A., Longo, E., Leite, E. R.** Room Temperature co-Precipitation of Nanocrystalline CeO_2 and $\text{Ce}_{0.8}\text{Gd}_{0.2}\text{O}_{1.9-8}$ Powder *Materials Letters* 2006 (in press).
2. **Zhang, T. S., Ma, J., Luo, L. H., Chan, S. H.** Preparation and Properties of Dense $\text{Ce}_{0.9}\text{Gd}_{0.1}\text{O}_{2-8}$ Ceramics for Use as Electrolytes in IT-SOFCs *Journal of Alloys and Compounds* 422 2006: pp. 46 – 52.
3. **Jigui Cheng, Shaowu Zha, Xiaohong Fang, Xingqin Liu, Guangyao Meng.** On the Green Density, Sintering Behavior and Electrical Property of Tape Cast $\text{Ce}_{0.9}\text{Gd}_{0.1}\text{O}_{1.95}$ Electrolyte Films *Materials Research Bulletin* 37 2002: pp. 2437 – 2446.
4. **Namjin Kim, Byong-Ho Kim, Dokyol Lee.** Effect of co-Dopant Addition on Properties of Gadolinia-Doped Ceria Electrolyte *Journal of Power Sources* 90 2000: pp. 139 – 143.
5. **Changrong Xia, Meilin Liu.** Microstructures, Conductivities, and Electrochemical Properties of $\text{Ce}_{0.9}\text{Gd}_{0.1}\text{O}_2$ and GDC–Ni Anodes for Low-Temperature SOFCs *Solid State Ionics* 152–153 2002: pp. 423 – 430.
6. **Ji-Gui Cheng, Shao-Wu Zha, Jia Huang, Xing-Qin Liu, Guang-Yao Meng.** Sintering Behavior and Electrical Conductivity of $\text{Ce}_{0.9}\text{Gd}_{0.1}\text{O}_{1.95}$ Powder Prepared by the Gel-Casting Process *Materials Chemistry and Physics* 78 2003: pp. 791 – 795.
7. **Shaowu Zha, William Rauch, Meilin Liu.** Ni- $\text{Ce}_{0.9}\text{Gd}_{0.1}\text{O}_{1.95}$ Anode for GDC Electrolyte-Based Low-Temperature SOFCs *Solid State Ionics* 166 2004: pp. 241 – 250.
8. **Song, H. Z., Wang, H. B., Zha, S. W., Peng, D. K., Meng, G. Y.** Aerosol-assisted MOCVD Growth of Gd_2O_3 -doped CeO_2 Thin SOFC Electrolyte Film on Anode Substrate *Solid State Ionics* 156 2003: pp. 249 – 254.
9. **Fergus, J. W.** Electrolytes for Solid Oxide Fuel Cells *Journal of Power Sources* 2006 (in press).
10. **Pederson, L. R., Singh, P., Zhou, X.-D.** Application of Vacuum Deposition Methods to Solid Oxide Fuel Cells *Vacuum* 80 2006: pp. 1066 – 1083.
11. **Laukaitis, G., Dudonis, J.** Development of SOFC Thin Film Electrolyte Using Electron Beam Evaporation Technique from the Cubic Phase YSZ Powder *Materials Science (Medžiagotyra)* 11 (1) 2005: pp. 9 – 13.
12. **Laukaitis, G., Dudonis, J., Milcius, D.** YSZ Thin Films Deposited by e-beam Technique *Thin Solid Films* 515 2006: pp. 678 – 682.
13. **Cheary, R. W., Coelho, A. A.** Programs XFIT and FOURYA, deposited in CCP14 Powder Diffraction Library, Engineering and Physical Sciences Research Council, Daresbury Laboratory, Warrington, England, 1996. (<http://www.ccp14.ac.uk/tutorial/xfit-95/xfit.htm>)
14. **Johnson, P. C.** *Physics of Thin Films* 14 1989: p. 129.
15. **Stelzer, N. H. J., Schoonman, J.** Synthesis of Terbia-Doped Ytria-Stabilized Zirconia Thin Films by Electrostatic Spray Deposition (ESD) *J.Mater. Synth. Process* 4/6 1996: p. 429.
16. **Movchan, B. A., Demchishin, A. V.** Investigation of the Structure and Properties of Thick Vacuum-Deposited Films of Nickel, Titanium, Tungsten, Alumina and Zirconium Dioxide *Fiz. Met. Metalloved.* 28 (4) 1969: pp. 653 – 660.
17. **Thornton, J. A.** Influence of Apparatus Geometry and Deposition Conditions on the Structure and Topography *J. Vac. Sci. Technol.* 11 1974: pp. 666 – 670.
18. **Lintymer, J., Martin, N., Chappe, J.-M., Delobelle, P., Takadoum, J.** *Surface and Coatings Technology* 180–181 2004: pp. 26 – 32.

DOI: 10.5755/j02.ms.26277